fractal and fractional

MDPI

Article

Lyapunov-Based Partial Practical Generalized Mittag–Leffler Stability and Polynomial Fuzzy Observer Design for Tempered Fractional-Order Systems

Ayed R. A. Alanzi [1], Raouf Fakhfakh [1,*], Omar Naifar [2,3,*] and Abdellatif Ben Makhlouf [4,5]

[1] Department of Mathematics, College of Science, Jouf University, P.O. Box 2014, Sakaka 72388, Saudi Arabia; aralenzi@ju.edu.sa
[2] Control and Energy Management Laboratory, National School of Engineering of Sfax, University of Sfax, Sfax 3038, Tunisia
[3] Higher Institute of Applied Sciences and Technology of Kairouan, University of Kairouan, Kairouan 3100, Tunisia
[4] Mathematics Education Section, Faculty of Education and Arts, Sohar University, P.O. Box 44, Sohar 311, Oman; abdellatif.benmakhlouf@fss.usf.tn
[5] Department of Mathematics, Faculty of Sciences of Sfax, University of Sfax, Sfax 3029, Tunisia
* Correspondence: rfakhfakh@ju.edu.sa (R.F.); omar.naifar@enis.tn (O.N.)

Abstract

This paper develops a Lyapunov-based framework for the analysis of partial practical stability in tempered fractional-order systems described by the tempered ζ-Caputo derivative. In contrast with classical full-state stability concepts, the proposed approach focuses on practical generalized Mittag–Leffler stability with respect to a prescribed component of the state vector. Sufficient conditions are established in terms of a Lyapunov function and suitable comparison estimates, leading to a notion of practical uniform generalized Mittag–Leffler stability for substates. The theoretical results are then applied to the observer design problem for a class of tempered fractional-order polynomial fuzzy systems. By exploiting a block decomposition of the estimation error and using polynomial fuzzy observer gains, new sufficient conditions are derived to guarantee practical generalized Mittag–Leffler stability of the estimation error with respect to its first component. The observer synthesis is formulated through polynomial matrix inequalities and sum-of-squares conditions on an admissible operating region. A numerical example involving a 3-dimensional tempered fractional-order polynomial fuzzy system is provided to illustrate the proposed methodology. The simulations confirm the effectiveness of the developed observer and show that the error component of interest converges inside a small neighborhood of the origin in agreement with the theoretical estimates. Quantitatively, the first error component is driven to $|e_1(10)| \approx 1.22 \times 10^{-3}$, two orders of magnitude below the theoretical envelope (1.07×10^{-1}), while the kernel-boundedness diagnostic remains finite ($\sup_{\varsigma} K(\varsigma) \approx 1.59$). In contrast with existing full-state Mittag–Leffler observer designs for fractional and tempered fuzzy systems, the proposed partial formulation certifies convergence of only the substate of interest and therefore requires the synthesis of a single observer-gain block. The obtained results contribute to the stability theory of tempered fractional-order systems and provide a constructive framework for partial-state observer design in nonlinear fuzzy settings.

Keywords: tempered ζ-Caputo derivative; partial practical stability; generalized Mittag–Leffler stability; polynomial fuzzy observer design; sum-of-squares

MSC: 34A08; 34A34; 93B07; 93C10; 93D05; 93D09

Check for updates

Academic Editors: Gustavo Ceballos-Benavides and Manuel A. Duarte-Mermoud

Received: 9 August 2026
Accepted: 27 August 2026
Published: 1 September 2026

Copyright: © 2026 by the authors. Licensee MDPI, Basel, Switzerland. This article is an open access article distributed under the terms and conditions of the Creative Commons Attribution (CC BY) license.

1. Introduction

Fractional calculus has become an important framework for modeling dynamical systems with memory, hereditary effects, and nonlocal behavior. Compared with classical integer-order models, fractional-order formulations often provide a more accurate description of complex phenomena arising in engineering, physics, biology, and applied sciences; see, for instance, the classical monographs [1,2] and the survey [3]. Over the last decades, fractional-order models have been successfully used in many applications, including epidemiological modeling, viscoelasticity, thermal processes, and control engineering [4,5]. Recent contributions further highlight the modeling power of fractional operators, ranging from theoretical analyses of delay fractional differential equations via fixed-point techniques [6] to numerical studies of fractional models in biological and tissue-transport settings [7,8]. In parallel, the stability theory of fractional-order systems has received considerable attention, especially in connection with Mittag–Leffler stability and Lyapunov-based methods [9].

Among the various fractional operators proposed in the literature, tempered fractional derivatives have attracted growing interest because they preserve the memory effects of fractional calculus while introducing an exponential tempering mechanism that better captures finite-memory phenomena. This feature makes tempered operators particularly suitable for describing systems in which long-range memory gradually decays over time. Recent developments have established generalized Laplace-transform tools, theoretical properties, and well-posedness results for tempered fractional differential equations [10–12]. In the control context, tempered fractional systems have also been investigated from the viewpoints of stability, stabilization, controllability, observability, and numerical approximation [13–16]. These developments confirm that tempered fractional calculus provides a flexible and practically relevant setting for modern system analysis.

Stability remains one of the central issues in the analysis and control of nonlinear systems. In many practical situations, however, asymptotic convergence to the origin is too restrictive, and weaker notions such as practical stability provide a more realistic framework. Practical stability has a long and rich history in control theory and nonlinear dynamical systems [17–19]. More recently, the notion of *partial* practical stability has been introduced to address systems in which only a subset of the state variables needs to be stabilized or estimated, while the remaining components may play the role of auxiliary or internal dynamics [20]. Such a viewpoint is especially meaningful in observer design, tracking, and output regulation, where the objective often concerns only a specific error component rather than the full state vector [21,22]. In the tempered fractional framework, Lyapunov-based criteria for practical stability and partial practical stability have only recently begun to emerge [13,23].

Observer design for fractional-order systems is another active research direction, motivated by the need to estimate unmeasured states in nonlinear and uncertain environments. Important advances have been reported for nonlinear Caputo fractional-order systems, robust and non-fragile observers, and observer-based control strategies [24]. In the fuzzy and polynomial fuzzy settings, observer design is particularly appealing because Takagi–Sugeno and polynomial fuzzy models allow one to approximate nonlinear dynamics by convex combinations of simpler local models. Recent contributions include observer design for fractional-order polynomial fuzzy systems depending on parameters [25], H_∞ observer-based control for fuzzy fractional-order systems [26], and fractional-order Thau–Luenberger observers for Takagi–Sugeno systems with uncertainties and unknown inputs [27]. In the tempered fractional setting, practical stabilization of nonlinear fuzzy systems and SOS-based stabilization of tempered fractional-order power systems have also been investigated [28,29]. More broadly, Lyapunov-based design lies at the heart of a wide

range of modern nonlinear control technologies, including adaptive, sliding-mode and terminal sliding-mode schemes for safety-critical plants such as nuclear power systems, where a suitably constructed Lyapunov function simultaneously certifies robustness against lumped disturbances and practical/finite-time convergence of the regulated variables [30]. The present study adopts the same Lyapunov philosophy, but in the tempered ζ-Caputo fractional setting and for the partial (substate) estimation problem. Nevertheless, despite these advances, the literature on *partial practical generalized Mittag–Leffler stability* for tempered fractional-order polynomial fuzzy observer error systems remains very limited.

Motivated by the above observations, this paper develops a Lyapunov-based framework for the analysis of partial practical stability in tempered fractional-order systems and applies it to polynomial fuzzy observer design. The first contribution is the establishment of sufficient conditions for partial practical generalized Mittag–Leffler stability with respect to a substate, within the class of nonlinear tempered fractional-order systems written in terms of the tempered ζ-Caputo derivative. The second contribution is the application of this general result to a class of polynomial fuzzy observer error systems, where the state is naturally decomposed into a component of interest and an auxiliary component. In this way, the proposed framework extends classical practical stability ideas [17,19,20] to the tempered fractional setting while also connecting with modern observer-design methods for fuzzy fractional systems [24–27]. Finally, a numerical example is provided to demonstrate the effectiveness of the proposed observer design and to illustrate the practical generalized Mittag–Leffler convergence of the estimation error component of interest. The numerical implementation is consistent with recent developments in tempered fractional numerical analysis [11,15,16].

The innovation and validity of this work can therefore be summarized as follows. On the theoretical side, to the best of our knowledge, it provides the first Lyapunov-based criterion for *partial* practical generalized Mittag–Leffler stability of tempered ζ-Caputo systems, i.e., stability with respect to a prescribed substate rather than the full state. On the methodological side, it turns this criterion into a *constructive* polynomial fuzzy observer design whose conditions reduce to sum-of-squares/polynomial matrix inequalities that are checkable offline on a compact operating region. The validity of both contributions is supported analytically (rigorous proofs of Theorems 1 and 2) and numerically (a three-dimensional example in which the certified error component stays well inside the predicted decay envelope).

The remainder of the paper is organized as follows. Section 2 recalls the main preliminaries on tempered ζ-fractional operators and Mittag–Leffler functions. Section 4 develops the polynomial fuzzy observer design and establishes the partial practical generalized Mittag–Leffler stability of the estimation error. Section 5 presents a numerical example illustrating the theoretical results. Concluding remarks are given in the final section.

Notation

For the convenience of the reader, the main symbols used throughout the paper are collected here. $\mathbb{R}^n$ is the n-dimensional Euclidean space, and $\|\cdot\|$ is the associated Euclidean norm; $\mathbb{R}_+ = [0,\infty)$; $\mathbb{S}^{n\times n}$ denotes the set of real symmetric $n \times n$ matrices. For a matrix P, $P = P^T > 0$ means that P is symmetric positive definite, and $\lambda_{\min}(P)$, $\lambda_{\max}(P)$ are its smallest and largest eigenvalues; I is the identity matrix and $(\cdot)^T$ denotes transposition. $C[b,c]$, $C^1[b,c]$ and $AC[b,c]$ are the spaces of continuous, continuously differentiable and absolutely continuous functions on $[b,c]$. $\Gamma(\cdot)$ is the Gamma function, and $E_{s_1,s_2}(\cdot)$, $E_{s_1}(\cdot)$ are the two- and one-parameter Mittag–Leffler functions. The operators $I_{b^+}^{\theta,\vartheta,\zeta}$ and ${}^{C}D_{b^+}^{\theta,\vartheta,\zeta}$ are the tempered ζ-fractional integral and the tempered ζ-Caputo derivative of order $\theta \in (0,1)$, with tempering parameter $\vartheta \geq 0$ and smooth increasing kernel $\zeta \in C^1$, $\zeta' > 0$.

The state is decomposed as $\beta = (\beta^1, \beta^2)$ (respectively $x = (x^1, x^2)$, $e = (e^1, e^2)$) into a component of interest and an auxiliary component, with $\beta^1 \in \mathbb{R}^{n_1}$, $\beta^2 \in \mathbb{R}^{n_2}$ and $n_1 + n_2 = n$. Here, $\omega > 0$ is a small parameter, $\mu(\cdot) \geq 0$ is a bounding function, $\beta_s(\cdot)$ are the fuzzy membership functions, and the notation "$p \in$ SOS" means that the polynomial p is a sum of squares.

2. Preliminaries

This section presents fundamental results pertaining to the tempered ζ-fractional integral and derivative. Here $\theta \in (0,1)$ is the fractional order, $\vartheta \geq 0$ is the tempering rate, and $\zeta \in C^1$ with $\zeta' > 0$ is a smooth increasing kernel that plays the role of a (possibly nonlinear) time scale; the classical tempered Caputo setting is recovered when $\zeta(\varsigma) = \varsigma$. These tempered ζ-operators, together with the associated generalized Laplace transform and comparison machinery, have been developed and exploited in a number of recent works [10–14]. For the underlying Lyapunov and Mittag–Leffler stability tools used in the sequel, we further refer to [3,9,23] and the references therein.

Definition 1 ([10]). *Suppose $\theta > 0$, $\vartheta \geq 0$, and let $y(\varsigma)$ belong to $C[b,c]$ while $\zeta(\varsigma) \in C^1[b,c]$ satisfies $\zeta'(\varsigma) > 0$ for all $\varsigma \in [b,c]$. Under these conditions, the tempered ζ-fractional integral of $y(\varsigma)$ of order θ is given by:*

$$I_{b^+}^{\theta,\vartheta,\zeta} y(\varsigma) = \frac{1}{\Gamma(\theta)} \int_b^{\varsigma} (\zeta(\varsigma) - \zeta(s))^{\theta-1} \exp\big(-\vartheta(\zeta(\varsigma) - \zeta(s))\big)\zeta'(s) y(s) ds.$$

Definition 2 ([10]). *Take $0 < \theta < 1$, $\vartheta \geq 0$, $\zeta(\varsigma) \in C^1[b,c]$ with $\zeta'(\varsigma) > 0$ throughout $[b,c]$, and $y(\varsigma) \in AC[b,c]$. Then, one defines the tempered ζ-Caputo fractional derivative of y of order θ by:*

$${}^{C}D_{b^+}^{\theta,\vartheta,\zeta} y(\varsigma) = \frac{\exp(-\vartheta\zeta(\varsigma))}{\Gamma(1-\theta)} \int_b^{\varsigma} (\zeta(\varsigma) - \zeta(s))^{-\theta} \frac{d}{ds}\big(\exp(\vartheta\zeta(s)) y(s)\big) ds. \tag{1}$$

Definition 3 ([10]). *The Mittag–Leffler function takes the form*

$$E_{s_1,s_2}(t) = \sum_{n=0}^{+\infty} \frac{t^n}{\Gamma(n s_1 + s_2)},$$

where the parameters satisfy $s_1 > 0$ and $s_2 > 0$, and t is any complex number. In the particular situation $s_2 = 1$, we write $E_{s_1}(t)$ as a shorthand for $E_{s_1,1}(t)$.

Lemma 1 ([10]). *For $Q \in \mathbb{S}^{n\times n}$ and an absolutely continuous mapping $y : [d_1, d_2] \longrightarrow \mathbb{R}^n$, it follows that*

$${}^{C}D_{d_1^+}^{\theta,\vartheta,\zeta} y^T Q y(\varsigma) \leq 2y(\varsigma)^T Q\, {}^{C}D_{d_1^+}^{\theta,\vartheta,\zeta} y(\varsigma). \tag{2}$$

Lemma 2 ([10]). *Let the system*

$${}^{C}D_{a^+}^{\theta,\vartheta,\zeta} y(\varsigma) = my + d(\varsigma), \tag{3}$$

in which $y \in \mathbb{R}^n$. The solution can be expressed as follows:

$$\begin{aligned} y(\varsigma) &= \exp\big(-\vartheta(\zeta(\varsigma) - \zeta(a))\big) E_\theta\big(m(\zeta(\varsigma) - \zeta(a))^\theta\big) y(a) \\ &+ \int_a^{\varsigma} (\zeta(\varsigma) - \zeta(s))^{\theta-1} E_{\theta,\theta}\big(m(\zeta(\varsigma) - \zeta(s))^\theta\big)\zeta'(s) \exp\big(-\vartheta(\zeta(\varsigma) - \zeta(s))\big) d(s) ds. \end{aligned} \tag{4}$$

3. Generalized Practical Stability

We consider the following class of tempered fractional-order systems (TFOSs),

$$
\begin{gathered}
{}^{C}D^{\theta,\vartheta,\zeta}_{\varsigma_0^+}\beta(\varsigma) = G(\varsigma,\beta,\omega), \quad \varsigma \geq \varsigma_0, \\
\beta(\varsigma_0) = \beta_0 = (\beta_0^1, \beta_0^2), \\
\beta \in \mathbb{R}^n, \quad \beta = (\beta^1, \beta^2), \quad \beta^1 \in \mathbb{R}^{n_1}, \quad \beta^2 \in \mathbb{R}^{n_2}, \\
n_1 > 0,\ n_2 > 0,\ n_1 + n_2 = n,
\end{gathered}
$$

with $0 < \theta < 1$, $\vartheta \geq 0$, $\varsigma_0 \geq 0$, $\omega > 0$, and $G(\cdot,\cdot,\omega) : \mathbb{R}_+ \times \mathbb{R}^n \to \mathbb{R}^n$. Here, $G(\varsigma,\beta,\omega)$ is the (possibly nonlinear) vector field governing the dynamics, depending on time ς, state β, and the small parameter $\omega > 0$ introduced in the Notation section; ω quantifies the magnitude of the perturbations and of the off-diagonal coupling of the model, and its precise role and choice are analyzed in Section Discussion: Design Parameters and Structural Assumptions. Here, the initial condition is split consistently with the state as $\beta_0 = (\beta_0^1, \beta_0^2)$, where $\beta_0^1 \in \mathbb{R}^{n_1}$ is the initial value of the substate of interest β^1, and $\beta_0^2 \in \mathbb{R}^{n_2}$ is the initial value of the auxiliary substate β^2 (the superscripts 1, 2 are block indices, not exponents).

Definition 4. *System (5) is called ω^*-ζ-practically uniformly generalized Mittag–Leffler stable with respect to β^1 (denoted ω^*-ζ-PUGMLS-β^1) if for every $0 < \omega \leq \omega^*$, there exist positive constants $d_1(\omega), d_2(\omega), d_3(\omega), d_4(\omega)$ such that for all $\varsigma \geq \varsigma_0 \geq 0$,*

$$
\|\beta^1_\omega(\varsigma;\varsigma_0,\beta_0)\| \leq d_1(\omega)\|\beta_0\| e^{-d_2(\omega)(\zeta(\varsigma)-\zeta(\varsigma_0))}\Big[E_\theta\big(-d_3(\omega)(\zeta(\varsigma)-\zeta(\varsigma_0))^\theta\big)\Big]^q + d_4(\omega), \tag{5}
$$

where $q > 0$, $d_4(\omega) \to 0$ as $\omega \to 0^+$, and there exist constants $H, c_1, c_2, b_1, b_2 > 0$ such that for all $\omega \in (0,\omega^*]$:

$$
0 < d_1(\omega) \leq H, \quad c_1 < d_2(\omega) < c_2, \quad b_1 \leq d_3(\omega) \leq b_2.
$$

In words, $d_1(\omega)$ is the transient-amplitude gain, $d_2(\omega)$ the exponential tempering rate, $d_3(\omega)$ the Mittag–Leffler decay rate, $q > 0$ a fixed power, and $d_4(\omega)$ is the radius of the ultimate residual ball, which vanishes as $\omega \to 0^+$; the constants H, c_1, c_2, b_1, b_2 make these bounds uniform in ω.

Theorem 1. *Let $\iota \geq 1$ and $\omega^* > 0$. Assume that for each $0 < \omega \leq \omega^*$, there exist*

- *a C^1 function $V_\omega : \mathbb{R}_+ \times \mathbb{R}^n \to \mathbb{R}$;*
- *a continuous function $\mu : \mathbb{R}_+ \to \mathbb{R}_+$;*
- *positive coefficients $a_1(\omega), a_2(\omega), a_3(\omega), r_1(\omega), r_2(\omega)$.*

This satisfies the following conditions:

(i)

$$
a_1(\omega)\|\beta^1\|^\iota \leq V_\omega(\varsigma,\beta) \leq a_2(\omega)\|\beta\|^\iota + r_1(\omega), \quad \forall \varsigma \geq 0,\ \beta \in \mathbb{R}^n. \tag{6}
$$

(ii)

$$
{}^{C}D^{\theta,\vartheta,\zeta}_{\varsigma_0^+}V_\omega(\varsigma,\beta_\omega(\varsigma;\varsigma_0,\beta_0)) \leq -a_3(\omega)\|\beta^1_\omega(\varsigma;\varsigma_0,\beta_0)\|^\iota + \mu(\varsigma)r_2(\omega), \quad \forall \varsigma \geq \varsigma_0. \tag{7}
$$

(iii)

For all $\omega \in (0,\omega^*]$,

$$
\frac{a_3(\omega)}{a_2(\omega)} \geq \alpha, \qquad 0 < \frac{a_2(\omega)}{a_1(\omega)} \leq K,
$$

with $\alpha, K > 0$ independent of ω.

(iv)
The map

$$\varsigma \mapsto \int_0^{\varsigma} (\zeta(\varsigma) - \zeta(l))^{\theta-1} \exp\big(-\vartheta(\zeta(\varsigma) - \zeta(l))\big) E_{\theta,\theta}\Big(-\alpha(\zeta(\varsigma) - \zeta(l))^{\theta}\Big) \zeta'(l)\mu(l)\, dl$$

is bounded over $\varsigma \geq 0$.

(v) *Let*

$$c(\omega) = r_1(\omega)\frac{a_2(\omega) + Ca_3(\omega)}{a_1(\omega)a_2(\omega)} + r_2(\omega)\frac{C}{a_1(\omega)},$$

where $C = C_1 + C_2$, *with*

$$C_1 = \sup_{s\geq 0}\Big(s^{\theta} E_{\theta,\theta+1}(-\alpha s^{\theta})\Big),$$

$$C_2 = \sup_{\varsigma\geq 0} \int_0^{\varsigma} (\zeta(\varsigma) - \zeta(l))^{\theta-1} \exp\big(-\vartheta(\zeta(\varsigma) - \zeta(l))\big) E_{\theta,\theta}\Big(-\alpha(\zeta(\varsigma) - \zeta(l))^{\theta}\Big) \zeta'(l)\mu(l)\, dl.$$

We require $c(\omega) \to 0$ *as* $\omega \to 0^+$.

Then, system (5) is ω^*-ζ-PUGMLS-β^1.

Proof. From (6) and (7), we obtain

$$\begin{aligned} {}^{C}D^{\theta,\vartheta,\zeta}_{\varsigma_0^+} V_\omega &\leq -\frac{a_3(\omega)}{a_2(\omega)} V_\omega(\varsigma, \beta_\omega) + \big(1 + \mu(\varsigma)\big) l(\omega) \\ &\leq -\alpha V_\omega(\varsigma, \beta_\omega) + \rho(\varsigma) l(\omega), \quad \varsigma \geq \varsigma_0, \end{aligned} \tag{8}$$

where $\rho(\varsigma) = 1 + \mu(\varsigma)$ and $l(\omega) = r_2(\omega) + \dfrac{r_1(\omega)a_3(\omega)}{a_2(\omega)}$.

Define

$$h(\varsigma) = {}^{C}D^{\theta,\vartheta,\zeta}_{\varsigma_0^+} V_\omega(\varsigma, \beta_\omega) + \alpha V_\omega(\varsigma, \beta_\omega). \tag{9}$$

Applying the solution representation from Lemma 2, we get

$$\begin{aligned} V_\omega(\varsigma, \beta_\omega) &= e^{-\vartheta(\zeta(\varsigma)-\zeta(\varsigma_0))} E_\theta\big(-\alpha(\zeta(\varsigma) - \zeta(\varsigma_0))^{\theta}\big) V_\omega(\varsigma_0, \beta_0) \\ &\quad + \int_{\varsigma_0}^{\varsigma} (\zeta(\varsigma) - \zeta(l))^{\theta-1} e^{-\vartheta(\zeta(\varsigma)-\zeta(l))} \\ &\quad \times E_{\theta,\theta}\Big(-\alpha(\zeta(\varsigma) - \zeta(l))^{\theta}\Big) \zeta'(l) h(l)\, dl. \end{aligned} \tag{10}$$

Using $h(s) \leq \rho(s) l(\omega)$ from (8) and (9), we obtain the bound

$$\begin{aligned} V_\omega(\varsigma, \beta_\omega) \leq\ & e^{-\vartheta(\zeta(\varsigma)-\zeta(\varsigma_0))} E_\theta\big(-\alpha(\zeta(\varsigma) - \zeta(\varsigma_0))^{\theta}\big) V_\omega(\varsigma_0, \beta_0) \\ & + Cl(\omega), \quad \forall \varsigma \geq \varsigma_0. \end{aligned} \tag{11}$$

Now, from the left inequality in (6),

$$\|\beta^1_\omega(\varsigma; \varsigma_0, \beta_0)\|^{\iota} \leq \frac{1}{a_1(\omega)} V_\omega(\varsigma, \beta_\omega).$$

Substituting (11) and the upper bound $V_\omega(\varsigma_0, \beta_0) \leq a_2(\omega)\|\beta_0\|^{\iota} + r_1(\omega)$ yields

$$\|\beta^1_\omega\|^{\iota} \leq \frac{1}{a_1(\omega)} e^{-\vartheta\Delta\zeta} E_\theta(-\alpha\Delta\zeta^{\theta})\big(a_2(\omega)\|\beta_0\|^{\iota} + r_1(\omega)\big) + \frac{Cl(\omega)}{a_1(\omega)}, \tag{12}$$

with $\Delta\zeta = \zeta(\varsigma) - \zeta(\varsigma_0)$. Since the exponential and Mittag–Leffler functions are bounded by 1, it follows that

$$\|\beta_\omega^1\|^\iota \leq \frac{a_2(\omega)}{a_1(\omega)} e^{-\vartheta\Delta\zeta} E_\theta(-\alpha\Delta\zeta^\theta)\|\beta_0\|^\iota + c(\omega). \tag{13}$$

We emphasize that the bound by 1 is applied *only* to absorb the constant term $\frac{1}{a_1(\omega)} e^{-\vartheta\Delta\zeta} E_\theta(-\alpha\Delta\zeta^\theta)\, r_1(\omega)$ into the residual $c(\omega)$. The decaying composite factor $e^{-\vartheta\Delta\zeta}\left[E_\theta(-\alpha\Delta\zeta^\theta)\right]$ is retained explicitly in the leading term of (13); hence, the exponential tempering and the Mittag–Leffler decay required in Definition 4 are fully preserved in the final estimate (14) and are not discarded.

Taking the ι-th root and applying an elementary inequality $(x+y)^{1/\iota} \leq x^{1/\iota} + y^{1/\iota}$ for $x, y \geq 0$, we get

$$\|\beta_\omega^1\| \leq \left(\frac{a_2(\omega)}{a_1(\omega)}\right)^{1/\iota} \|\beta_0\| e^{-\frac{\vartheta}{\iota}\Delta\zeta}\left[E_\theta\big(-\alpha\Delta\zeta^\theta\big)\right]^{1/\iota} + r(\omega), \tag{14}$$

where $r(\omega) = c(\omega)^{1/\iota}$. This matches the required stability estimate, completing the proof. □

Remark 1. *(Simple sufficient criterion for condition (iv).) Conditions (iv) and (v) of Theorem 1 involve the boundedness of a tempered Mittag–Leffler convolution kernel, which may look difficult to verify directly. In fact, it is automatically satisfied whenever the comparison function μ is bounded on $\mathbb{R}_+$, i.e., $\mu(\varsigma) \leq \bar{\mu} < \infty$ for all $\varsigma \geq 0$. This covers, in particular, constant, bounded, and exponentially decreasing μ. Indeed, using $e^{-\vartheta(\zeta(\varsigma)-\zeta(l))} \leq 1$, the positivity of $E_{\theta,\theta}(-\alpha u^\theta)$ for $\theta \in (0,1)$, and the substitution $u = \zeta(\varsigma) - \zeta(l)$ (so that $du = \zeta'(l)\, dl$),*

$$\begin{aligned}\int_0^\varsigma (\zeta(\varsigma)-\zeta(l))^{\theta-1} e^{-\vartheta(\zeta(\varsigma)-\zeta(l))} E_{\theta,\theta}\big(-\alpha(\zeta(\varsigma)-\zeta(l))^\theta\big)\zeta'(l)\,\mu(l)\,dl &\leq \bar{\mu}\int_0^{\Delta\zeta_0} u^{\theta-1} E_{\theta,\theta}(-\alpha u^\theta)\,du \\ &= \frac{\bar{\mu}}{\alpha}\Big(1 - E_\theta(-\alpha\,\Delta\zeta_0^\theta)\Big) \leq \frac{\bar{\mu}}{\alpha},\end{aligned}$$

with $\Delta\zeta_0 = \zeta(\varsigma) - \zeta(0)$, where we used the identity $\int_0^z u^{\theta-1} E_{\theta,\theta}(-\alpha u^\theta)\, du = \alpha^{-1}\big(1 - E_\theta(-\alpha z^\theta)\big)$. Hence, the kernel map is uniformly bounded by $\bar{\mu}/\alpha$ and $C_2 \leq \bar{\mu}/\alpha$, so condition (iv) holds with no further verification. In the polynomial fuzzy observer of Section 4, μ is bounded on the compact operating region, so this criterion applies.

4. Application to Polynomial Fuzzy Observer Design

In this section, we design a polynomial fuzzy observer for a class of tempered fractional-order nonlinear systems and use Theorem 1 to establish the practical generalized Mittag–Leffler stability of the estimation error with respect to its first component.

We consider a class of tempered fractional-order polynomial fuzzy systems with state decomposition

$$x(\varsigma) = \big(x^1(\varsigma), x^2(\varsigma)\big) \in \mathbb{R}^{n_1} \times \mathbb{R}^{n_2}, \qquad n_1 > 0, \quad n_2 > 0, \quad n_1 + n_2 = n,$$

where $x^1(\varsigma)$ denotes the state component of interest, and $x^2(\varsigma)$ is regarded as an auxiliary internal dynamics.

Model rule s ($s \in \mathcal{S} = \{1, 2, \ldots, f\}$):

If $N_1(\varsigma)$ is Q_{s1} and $\cdots$ and $N_p(\varsigma)$ is Q_{sp}, *then*

$$
\begin{aligned}
{}^{C}D^{\theta,\vartheta,\zeta}_{\varsigma_0^+} x^1(\varsigma) &= A_s^{11}(y(\varsigma))x^1(\varsigma) + A_s^{12}(y(\varsigma))x^2(\varsigma) + \phi_s^1(\varsigma, x(\varsigma), \omega), && (15)\\
{}^{C}D^{\theta,\vartheta,\zeta}_{\varsigma_0^+} x^2(\varsigma) &= A_s^{21}(y(\varsigma))x^1(\varsigma) + A_s^{22}(y(\varsigma))x^2(\varsigma) + \phi_s^2(\varsigma, x(\varsigma), \omega), && (16)\\
y(\varsigma) &= C_1 x^1(\varsigma),
\end{aligned}
$$

where $u(\varsigma)$ is omitted for simplicity of exposition, since it does not affect the error analysis, $y(\varsigma) \in \mathbb{R}^p$ is the measured output, $C_1 \in \mathbb{R}^{p\times n_1}$ is a constant output matrix, and the matrices $A_s^{ij}(y(\varsigma))$ are polynomial in the measurable output $y(\varsigma)$.

The overall polynomial fuzzy model is written as

$$
{}^{C}D^{\theta,\vartheta,\zeta}_{\varsigma_0^+} x(\varsigma) = \sum_{s=1}^{f} \beta_s(N(\varsigma))(A_s(y(\varsigma))x(\varsigma) + \phi_s(\varsigma, x(\varsigma), \omega)), \tag{17}
$$

where

$$
A_s(y) = \begin{bmatrix} A_s^{11}(y) & A_s^{12}(y) \\ A_s^{21}(y) & A_s^{22}(y) \end{bmatrix}, \qquad \phi_s = \begin{bmatrix} \phi_s^1 \\ \phi_s^2 \end{bmatrix},
$$

and the membership functions satisfy

$$
\beta_s(N(\varsigma)) \geq 0, \qquad \sum_{s=1}^{f} \beta_s(N(\varsigma)) = 1.
$$

The polynomial fuzzy plant rules (15) and (16) are obtained from the original nonlinear tempered fractional-order model by the standard sector-nonlinearity (Takagi–Sugeno) construction: the measurable nonlinear terms of the plant are taken as the premise variables $N_1, \ldots, N_p$, and the membership functions β_s are built so that $\beta_s \geq 0$ and $\sum_s \beta_s = 1$, which makes the fuzzy model an exact convex (polytopic) representation of the plant on the operating region rather than an approximation. The observer rules (20) and (21) are then chosen by the parallel-distributed-compensation (PDC) principle: each observer rule copies the dynamics of the corresponding plant rule and adds an output-injection term $L_s(y)(y - \hat{y})$ sharing the same premises β_s. Regarding Assumption 1, conditions (H1) and (H3) hold by construction, because the premises and the matrices A_s^{ij} are formed only from measured signals; (H2) holds because the perturbations ϕ_s are smooth, and the model is evaluated on the *compact* region $\mathcal{Y}$, on which smooth functions are globally Lipschitz, with constants of order ω since ϕ_s and the off-diagonal coupling A_s^{12} scale with ω; (H4) is enforced by choosing $\mathcal{Y}$ as a compact set containing the output trajectory, which is verified *a posteriori* in Section 5 ($\max_\varsigma |y(\varsigma)| = 1 < 2$). Hence, Assumption 1 is not restrictive and can be guaranteed constructively for this class of models.

We assume the following.

Assumption 1. *The following conditions hold:*

(H1) The matrices $A_s^{ij}(y(\varsigma))$, $i, j \in \{1, 2\}$ *depend only on measurable variables.*

(H2) For each $s \in \mathcal{S}$, *there exist continuous functions* $\mu_{1,s}, \mu_{2,s} : \mathbb{R}_+ \to \mathbb{R}_+$ *and positive functions* $\delta_{1,s}(\omega)$, $\delta_{2,s}(\omega)$ *such that, for all* $\varsigma \geq \varsigma_0$ *and all* $x, \hat{x} \in \mathbb{R}^n$,

$$
\|\phi_s^1(\varsigma, x, \omega) - \phi_s^1(\varsigma, \hat{x}, \omega)\| \leq \delta_{1,s}(\omega)\|x^1 - \hat{x}^1\| + \delta_{2,s}(\omega)\mu_{1,s}(\varsigma), \tag{18}
$$

and

$$
\|A_s^{12}(y(\varsigma))(x^2 - \hat{x}^2)\| \leq \delta_{1,s}(\omega)\|x^1 - \hat{x}^1\| + \delta_{2,s}(\omega)\mu_{2,s}(\varsigma). \tag{19}
$$

Moreover,

$$\lim_{\omega\to 0^+}\delta_{1,s}(\omega)=0,\qquad \lim_{\omega\to 0^+}\delta_{2,s}(\omega)=0.$$

For simplicity, define the uniform bounds

$$\delta_1(\omega)=2\max_{s\in\mathcal{S}}\delta_{1,s}(\omega),\qquad \delta_2(\omega)=2\max_{s\in\mathcal{S}}\delta_{2,s}(\omega),$$

$$\mu(\varsigma)=\max_{s\in\mathcal{S}}\big(\mu_{1,s}(\varsigma)+\mu_{2,s}(\varsigma)\big).$$

(H3) The premise variables $N_j(\varsigma)$ and $j=1,\dots,p$ are measurable.
(H4) There exists a compact operating region $\mathcal{Y}\subset\mathbb{R}^p$ such that $y(\varsigma)\in\mathcal{Y}$ for all $\varsigma\geq\varsigma_0$.

Remark 2. *(On the coupling condition (19).) The term $A_s^{12}(y)(x^2-\hat{x}^2)$ is indeed part of the linear error dynamics and not an exogenous disturbance; (19) should be read as a structural smallness/boundedness condition on the off-diagonal coupling, not as a disturbance hypothesis. A simpler and fully equivalent sufficient condition is the matrix bound*

$$\|A_s^{12}(y)\|\leq\delta_{1,s}(\omega)\qquad \textit{for all } y\in\mathcal{Y},$$

since then $\|A_s^{12}(y)(x^2-\hat{x}^2)\|\leq\delta_{1,s}(\omega)\|x^2-\hat{x}^2\|$, and the bounded auxiliary error contributes the term $\delta_{2,s}(\omega)\mu_{2,s}(\varsigma)$. Equivalently, the coupling can be kept inside the Lyapunov inequality (32) as a structured term rather than passed through as a perturbation, leading to the same conclusion. This is exactly what happens in the numerical example, where $A_s^{12}(y)=\mathcal{O}(\omega)$, so that $\|A_s^{12}(y)\|\to 0$ as $\omega\to 0^+$, and the smallness requirement is met automatically.

We propose the following polynomial fuzzy observer.

Observer rule s ($s\in\mathcal{S}=\{1,2,\dots,f\}$):
If $N_1(\varsigma)$ is Q_{s1} and $\cdots$ and $N_p(\varsigma)$ is Q_{sp}, *then*

$$\begin{aligned}
{}^{C}D^{\theta,\vartheta,\zeta}_{\varsigma_0^+}\hat{x}^1(\varsigma) &= A_s^{11}(y(\varsigma))\hat{x}^1(\varsigma)+A_s^{12}(y(\varsigma))\hat{x}^2(\varsigma)+\phi_s^1(\varsigma,\hat{x}(\varsigma),\omega)\\
&\quad +L_s^1(y(\varsigma))\big(y(\varsigma)-\hat{y}(\varsigma)\big), \qquad (20)\\
{}^{C}D^{\theta,\vartheta,\zeta}_{\varsigma_0^+}\hat{x}^2(\varsigma) &= A_s^{21}(y(\varsigma))\hat{x}^1(\varsigma)+A_s^{22}(y(\varsigma))\hat{x}^2(\varsigma)+\phi_s^2(\varsigma,\hat{x}(\varsigma),\omega)\\
&\quad +L_s^2(y(\varsigma))\big(y(\varsigma)-\hat{y}(\varsigma)\big), \qquad (21)\\
\hat{y}(\varsigma) &= C_1\hat{x}^1(\varsigma),
\end{aligned}$$

where

$$L_s(y)=\begin{bmatrix}L_s^1(y)\\ L_s^2(y)\end{bmatrix}\in\mathbb{R}^{n\times p}$$

is the rule-dependent polynomial observer gain.

It is worth noting that the partial practical stability result established below only requires the design of the first gain block $L_s^1(y)$. The second block $L_s^2(y)$ may therefore be selected independently, for instance, set to zero or tuned to improve the transient behavior of the auxiliary error component e^2.

Let the estimation error be

$$e(\varsigma)=x(\varsigma)-\hat{x}(\varsigma)=\big(e^1(\varsigma),e^2(\varsigma)\big),$$

where

$$e^1(\varsigma)=x^1(\varsigma)-\hat{x}^1(\varsigma),\qquad e^2(\varsigma)=x^2(\varsigma)-\hat{x}^2(\varsigma).$$

Then, the first block of the estimation error satisfies

$$ {}^{C}D^{\theta,\vartheta,\zeta}_{\varsigma_0^+} e^1(\varsigma) = \sum_{s=1}^{f} \beta_s(N(\varsigma)) \Big((A_s^{11}(y(\varsigma)) - L_s^1(y(\varsigma))C_1)e^1(\varsigma) + A_s^{12}(y(\varsigma))e^2(\varsigma) + \widetilde{\phi}_s^1(\varsigma, e(\varsigma), \omega) \Big), \tag{22} $$

where

$$ \widetilde{\phi}_s^1(\varsigma, e, \omega) = \phi_s^1(\varsigma, x(\varsigma), \omega) - \phi_s^1(\varsigma, \hat{x}(\varsigma), \omega). \tag{23} $$

We now state a sufficient condition for polynomial fuzzy observer design.

Theorem 2. *Assume that Assumption 1 holds. Let $\eta > 0$ be a given scalar. Suppose that there exist a symmetric positive definite matrix $P \in \mathbb{R}^{n_1 \times n_1}$ and polynomial matrices $Y_s(y) \in \mathbb{R}^{n_1 \times p}$, $s = 1, \ldots, f$, such that*

$$ -\xi^T \Big(P A_s^{11}(y) - Y_s(y) C_1 + \big(A_s^{11}(y)\big)^T P - C_1^T Y_s^T(y) + \eta I \Big) \xi \in SOS, \tag{24} $$

for all $s \in \mathcal{S}$ and all admissible $y \in \mathcal{Y}$, where $\xi \in \mathbb{R}^{n_1}$ is a vector independent of y.

Assume also that the map

$$ \begin{aligned} \varsigma \mapsto \int_{\varsigma_0}^{\varsigma} & (\zeta(\varsigma) - \zeta(l))^{\theta-1} \exp\big(-\vartheta(\zeta(\varsigma) - \zeta(l)) \big) \\ & \times E_{\theta,\theta}\Big(-\frac{\eta}{2\lambda_{\max}(P)} (\zeta(\varsigma) - \zeta(l))^{\theta} \Big) \zeta'(l) \mu^2(l)\, dl \end{aligned} \tag{25} $$

is bounded on $[\varsigma_0, +\infty)$.

Then, with the first observer gain block defined by

$$ L_s^1(y(\varsigma)) = P^{-1} Y_s(y(\varsigma)), \qquad s = 1, \ldots, f, $$

there exists $\bar{\omega} \in (0, \omega^*]$ such that the estimation error system (22) is $\bar{\omega}$-ζ-practically uniformly generalized Mittag–Leffler stable with respect to e^1.

More precisely, for every $0 < \omega \le \bar{\omega}$ and every $\varsigma \ge \varsigma_0$, one has

$$ \|e^1(\varsigma)\| \le \sqrt{\frac{\lambda_{\max}(P)}{\lambda_{\min}(P)}} \|e^1(\varsigma_0)\| \exp\Big(-\frac{\vartheta}{2} \big(\zeta(\varsigma) - \zeta(\varsigma_0)\big) \Big) \left[E_{\theta}\Big(-\frac{\eta}{2\lambda_{\max}(P)} \big(\zeta(\varsigma) - \zeta(\varsigma_0)\big)^{\theta} \Big) \right]^{\frac{1}{2}} + r(\omega), \tag{26} $$

where

$$ r(\omega) = c(\omega)^{1/2}, \qquad r(\omega) \to 0 \quad as \quad \omega \to 0^+, $$

and $c(\omega)$ is the quantity defined in Theorem 1 corresponding to

$$ a_1(\omega) = \lambda_{\min}(P), \qquad a_2(\omega) = \lambda_{\max}(P), \qquad a_3(\omega) = \frac{\eta}{2}, $$

$$ r_1(\omega) = 0, \qquad r_2(\omega) = \frac{4\lambda_{\max}^2(P)}{\eta} \delta_2^2(\omega), $$

with the function μ replaced by μ^2.

Proof. Choose the Lyapunov function candidate

$$ V(e(\varsigma)) = (e^1(\varsigma))^T P e^1(\varsigma). $$

Since $P = P^T > 0$, we have

$$ \lambda_{\min}(P) \|e^1(\varsigma)\|^2 \le V(e(\varsigma)) \le \lambda_{\max}(P) \|e^1(\varsigma)\|^2. \tag{27} $$

In particular,

$$\lambda_{\min}(P)\|e^1(\varsigma)\|^2 \le V(e(\varsigma)) \le \lambda_{\max}(P)\|e(\varsigma)\|^2. \tag{28}$$

Using Lemma 1 and (22), one obtains

$$\begin{aligned} {}^{C}D^{\theta,\vartheta,\zeta}_{\varsigma_0^+}V(e(\varsigma)) &\le 2(e^1(\varsigma))^T P\, {}^{C}D^{\theta,\vartheta,\zeta}_{\varsigma_0^+}e^1(\varsigma) \\ &= \sum_{s=1}^{f}\beta_s(N(\varsigma))\Big(2(e^1)^T P(A_s^{11}(y)-L_s^1(y)C_1)e^1 + 2(e^1)^T PA_s^{12}(y)e^2 + 2(e^1)^T P\widetilde{\phi}_s^1(\varsigma,e,\omega)\Big). \end{aligned} \tag{29}$$

Since $L_s^1(y) = P^{-1}Y_s(y)$, we get

$$P(A_s^{11}(y)-L_s^1(y)C_1) = PA_s^{11}(y) - Y_s(y)C_1.$$

Hence,

$$2(e^1)^T P(A_s^{11}(y)-L_s^1(y)C_1)e^1 = (e^1)^T\Omega_s(y)e^1,$$

where

$$\Omega_s(y) = PA_s^{11}(y) - Y_s(y)C_1 + \big(A_s^{11}(y)\big)^T P - C_1^T Y_s^T(y).$$

From (24), we obtain

$$(e^1)^T\Omega_s(y)e^1 \le -\eta\|e^1\|^2, \qquad \forall s\in\mathcal{S},\ \forall y\in\mathcal{Y}.$$

On the other hand, from (18) and (19), together with the uniform bounds introduced in Assumption 1, we have

$$\|A_s^{12}(y)e^2 + \widetilde{\phi}_s^1(\varsigma,e,\omega)\| \le \delta_1(\omega)\|e^1\| + \delta_2(\omega)\mu(\varsigma).$$

Thus,

$$\begin{aligned} 2(e^1)^T P\big(A_s^{12}(y)e^2 + \widetilde{\phi}_s^1(\varsigma,e,\omega)\big) &\le 2\lambda_{\max}(P)\|e^1\|\|A_s^{12}(y)e^2 + \widetilde{\phi}_s^1(\varsigma,e,\omega)\| \\ &\le 2\lambda_{\max}(P)\delta_1(\omega)\|e^1\|^2 + 2\lambda_{\max}(P)\delta_2(\omega)\mu(\varsigma)\|e^1\|. \end{aligned} \tag{30}$$

Since $\delta_1(\omega)\to 0$ as $\omega\to 0^+$, there exists $\bar{\omega}\in(0,\omega^*]$ such that

$$2\lambda_{\max}(P)\delta_1(\omega) \le \frac{\eta}{4}, \qquad \forall\omega\in(0,\bar{\omega}]. \tag{31}$$

Moreover, by Young's inequality,

$$2\lambda_{\max}(P)\delta_2(\omega)\mu(\varsigma)\|e^1\| \le \frac{\eta}{4}\|e^1\|^2 + \frac{4\lambda_{\max}^2(P)}{\eta}\delta_2^2(\omega)\mu^2(\varsigma).$$

Substituting the above estimates into (29) yields

$${}^{C}D^{\theta,\vartheta,\zeta}_{\varsigma_0^+}V(e(\varsigma)) \le -\frac{\eta}{2}\|e^1(\varsigma)\|^2 + \frac{4\lambda_{\max}^2(P)}{\eta}\delta_2^2(\omega)\mu^2(\varsigma). \tag{32}$$

Therefore, the assumptions of Theorem 1 are satisfied with

$$\beta = e = (e^1,e^2), \qquad \iota = 2,$$

$$a_1(\omega) = \lambda_{\min}(P), \qquad a_2(\omega) = \lambda_{\max}(P), \qquad a_3(\omega) = \frac{\eta}{2},$$

$$r_1(\omega) = 0, \qquad r_2(\omega) = \frac{4\lambda_{\max}^2(P)}{\eta}\delta_2^2(\omega),$$

and

$$\alpha = \frac{a_3(\omega)}{a_2(\omega)} = \frac{\eta}{2\lambda_{\max}(P)}.$$

The ratio conditions in Theorem 1 are clearly satisfied. In addition, (25) is exactly the boundedness condition required in Theorem 1 with the function μ^2 in place of μ. Since $\delta_2(\omega) \to 0$ as $\omega \to 0^+$, we obtain $r_2(\omega) \to 0$, and therefore the quantity $c(\omega)$ of Theorem 1 tends to zero as $\omega \to 0^+$. Hence, by Theorem 1, the estimation error system (22) is $\bar{\omega}$-ζ-practically uniformly generalized Mittag–Leffler stable with respect to e^1, and estimate (26) holds. Since $\iota = 2$, the residual term is given by $r(\omega) = c(\omega)^{1/2}$. □

Remark 3. *Theorem 2 provides a polynomial fuzzy observer design procedure in the tempered ζ-Caputo framework. In contrast with a full-state quadratic analysis, the present result is genuinely partial: the Lyapunov function depends only on e^1, while the coupling term involving e^2 is absorbed into the vanishing perturbation term. The compact set $\mathcal{Y}$ represents the admissible operating region of the measured output, on which the SOS condition (24) is required to hold.*

Remark 4. *(Why (24) yields practical, and not asymptotic, stability.) The SOS condition (24) guarantees the negative-definite core $(e^1)^T\Omega_s(y)e^1 \le -\eta\|e^1\|^2$ of the Lyapunov inequality. Taken alone, this term would force V to zero and would yield asymptotic generalized Mittag–Leffler stability. However, the off-diagonal coupling and the nonlinearity add the term $\frac{4\lambda_{\max}^2(P)}{\eta}\delta_2^2(\omega)\mu^2(\varsigma)$ in (32), which does not vanish along the trajectory for a fixed $\omega > 0$. This residual prevents exact convergence to the origin and instead confines e^1 to a neighborhood of radius $r(\omega)$, i.e., practical stability. Since $\delta_2(\omega) \to 0$ as $\omega \to 0^+$, one has $r(\omega) \to 0$, and asymptotic generalized Mittag–Leffler stability is recovered in the limit. Hence, the negative definiteness in (24) fixes the decay rate, while the ω-dependent residual fixes the size of the practical neighborhood; the two statements are fully consistent.*

Remark 5. *(On the quadratic choice $\iota = 2$.) Theorem 1 is stated for a general exponent $\iota \ge 1$, so the partial practical generalized Mittag–Leffler framework is not intrinsically restricted to quadratic shapes. The quadratic Lyapunov function $V(e) = (e^1)^T Pe^1$ (i.e., $\iota = 2$) is adopted in Theorem 2 precisely because it converts the synthesis into the convex SOS/LMI test (24), which is efficiently solvable. Higher-order or non-quadratic Lyapunov candidates (for instance, $V = \|e^1\|^\iota$ with $\iota > 2$, or higher-degree polynomial/SOS Lyapunov functions) remain admissible under Theorem 1 and may further reduce conservatism at the cost of generally non-convex design conditions; this is a natural extension for future work.*

Remark 6. *(Computational complexity.) The procedure has two separable costs. Offline, one solves the SOS feasibility problem (24) once for P and the gain matrices Y_s; in the example, $n_1 = 1$, so (24) reduces to a single scalar polynomial inequality verified with margin on $\mathcal{Y}$ (the design polynomial remains in $[-6.4, -3.8] < 0$), while in general, it is a semidefinite program of size $\mathcal{O}(n_1)$, solvable in polynomial time by standard solvers such as SOSTOOLS. Online, the dominant cost is the integration of the tempered fractional dynamics: because fractional operators are nonlocal, the predictor–corrector scheme keeps the full solution history, giving an $\mathcal{O}(N^2)$ cost for N time steps ($N = 500$ here). For long horizons or higher-dimensional systems, this can be lowered to $\mathcal{O}(N \log N)$ or $\mathcal{O}(N)$ by short-memory truncation, FFT-based fast-convolution quadrature, or sum-of-exponentials/diffusive approximations of the tempered kernel, without affecting the offline gain synthesis.*

For practical implementation, the polynomial fuzzy observer design procedure given by Theorem 2 can be summarized as follows.

1. Determine the admissible operating region $\mathcal{Y}$ and verify Assumption 1. In particular, compute the uniform bounds $\delta_1(\omega)$, $\delta_2(\omega)$, and $\mu(\varsigma)$.
2. Solve the SOS condition (24) for $P = P^T > 0$ and the polynomial matrices $Y_s(y)$, $s = 1, \ldots, f$, for all $y \in \mathcal{Y}$. In practice, $\mathcal{Y}$ is described as a compact semialgebraic set; the SOS condition is sufficient, and it can be solved using standard software such as SOSTOOLS.
3. Compute the first observer gain block
$$L_s^1(y) = P^{-1}Y_s(y), \qquad s = 1, \ldots, f.$$
4. Choose the second observer gain block $L_s^2(y)$ independently, for instance, $L_s^2(y) = 0$, or tune it to improve the transient behavior of e^2.
5. Verify that the boundedness condition (25) holds. This condition depends only on P, η, and μ, and it is independent of ω, so it can be checked once.
6. Choose $\bar{\omega} \in (0, \omega^*]$ such that
$$2\lambda_{\max}(P)\delta_1(\omega) \leq \frac{\eta}{4}, \qquad \forall \omega \in (0, \bar{\omega}].$$
7. Implement the observer from (20) and (21).
8. Apply Theorem 2 to conclude that the estimation error is $\bar{\omega}$-ζ-practically uniformly generalized Mittag–Leffler stable with respect to e^1 and satisfies (26).

The above procedure provides a concise recipe for computing the polynomial observer gains and checking the assumptions required for the application of Theorem 2. Once these steps are fulfilled, the practical generalized Mittag–Leffler stability of the estimation error component e^1 follows directly. For the convenience of the reader, these eight steps are summarized in the flowchart of Figure 1.

Discussion: Design Parameters and Structural Assumptions

Role and choice of the small parameter ω**.** The parameter $\omega > 0$ has a precise mathematical meaning: it quantifies the magnitude of the vanishing nonlinear perturbations and of the off-diagonal coupling, since $\delta_1(\omega) \to 0$ and $\delta_2(\omega) \to 0$ as $\omega \to 0^+$ (in the example, ϕ_s and A_s^{12} are $\mathcal{O}(\omega)$). Thus, ω measures how far the plant is from the unperturbed, exactly observable case, and it controls the ultimate radius through $r(\omega) = c(\omega)^{1/2} \to 0$. The admissible range of ω is dictated by (31): the design tolerates every disturbance level up to the largest $\bar{\omega}$ for which $2\lambda_{\max}(P)\delta_1(\omega) \leq \eta/4$. Consequently, there is a monotone trade-off rather than an interior optimum: decreasing ω only shrinks the residual ball, while $\bar{\omega}$ is the largest disturbance the design can accommodate for the prescribed margin η. A practical "optimal" choice is therefore $\omega = \bar{\omega}$ when robustness to the largest admissible disturbance is sought, and a smaller ω when a tighter ultimate bound is the priority.

Choice of η **and its effect.** The scalar η sets the certified decay rate, since the Mittag–Leffler exponent in (26) is $\alpha = \eta/(2\lambda_{\max}(P))$, and it also shrinks the residual because $r_2(\omega) = 4\lambda_{\max}^2(P)\delta_2^2(\omega)/\eta$ decreases with η. Increasing η therefore speeds up convergence and tightens the ultimate bound. The price is feasibility: the SOS condition (24) requires $-\left(PA_s^{11} - Y_sC_1 + (A_s^{11})^TP - C_1^TY_s^T + \eta I\right)$ to be SOS, so a larger η must be dominated by the design and generally calls for larger gains Y_s (hence, larger L_s^1), until the test becomes infeasible beyond some $\eta_{\max}$. A systematic selection is, thus, to maximize η subject to SOS feasibility (a one-dimensional search/bisection on η). In the example, $\eta = 1$ keeps the design polynomial at most $-3.8 < 0$ on $\mathcal{Y}$, i.e., feasible with margin.

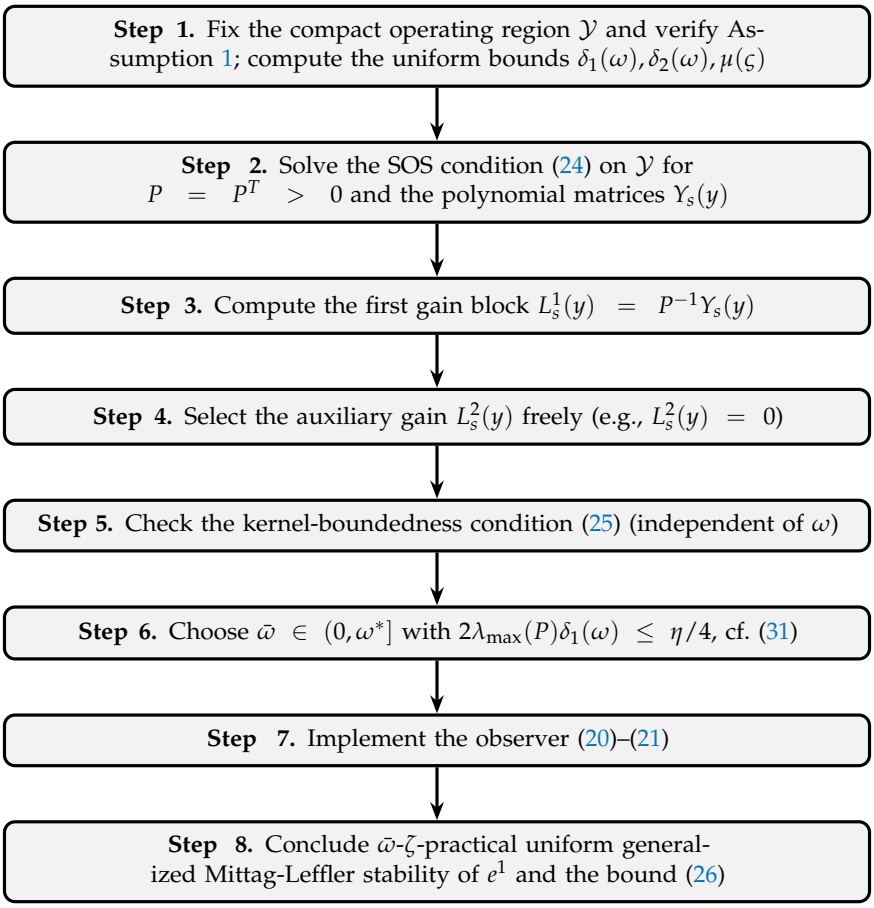

Figure 1. Flowchart summarizing the polynomial fuzzy observer design procedure (Steps 1–8).

Why the tempered ζ-Caputo derivative The kernel ζ replaces physical time with monotone intrinsic time $\zeta(\varsigma)$, so that memory accumulates on a possibly non-uniform clock. This single operator subsumes several classical ones ($\zeta(\varsigma) = \varsigma$ gives the standard tempered Caputo derivative, $\zeta(\varsigma) = \ln \varsigma$ gives a tempered Hadamard-type derivative, etc.), which is why we adopt the ζ-version rather than the plain tempered Caputo derivative: it yields a unified design valid for a whole family of memory kernels. The observer synthesis is form-invariant in ζ, but the performance is measured in ζ-time: the decay envelope in (26) is $e^{-\frac{\vartheta}{2}(\zeta(\varsigma)-\zeta(\varsigma_0))}\left[E_\theta(-\alpha(\zeta(\varsigma)-\zeta(\varsigma_0))^\theta)\right]^{1/2}$. Hence, a kernel growing faster than linear ($\zeta' > 1$) accelerates the real-time convergence of e^1, while a slowly growing kernel slows it down. The choice $\zeta(\varsigma) \neq \varsigma$ is therefore an additional modeling/tuning degree of freedom that is absent from the standard tempered Caputo setting.

Why the matrices A_s^{ij} depend only on the measured output. Requiring $A_s^{ij}(y)$ to depend solely on y (Assumption 1(H1)) is what makes the observer implementable and the certificate verifiable: the gains $L_s(y) = P^{-1}Y_s(y)$ and the memberships $\beta_s(N)$ must be computable online from measured signals, and the SOS condition (24) must be checkable on the measured region $\mathcal{Y}$. If the matrices depended on the unmeasured substate x^2, neither the gains nor the SOS certificate could be evaluated, and the polynomial inequalities would be posed over unmeasured variables. The assumption is, thus, essential for the present SOS route but not fundamental to the stability concept itself: it can be relaxed by bounding the unmeasured dependence as a structured uncertainty or by using descriptor/LPV embeddings at the cost of added conservatism, which we leave for future work.

Effect of the auxiliary gain L_s^2 on the error e^2. Although Theorem 2 only needs L_s^1, the auxiliary error obeys

$$ {}^{C}D_{\varsigma_0^+}^{\theta,\vartheta,\zeta} e^2 = \sum_{s=1}^{f} \beta_s(N) \Big(A_s^{21}(y) e^1 + A_s^{22}(y) e^2 + \widetilde{\phi}_s^2 - L_s^2(y) C_1 e^1 \Big). $$

With $L_s^2 = 0$, e^2 is a tempered fractional system with internal matrices A_s^{22}, driven by the practically vanishing e^1 and the perturbation. Hence, neglecting L_s^2 does *not* endanger e^2 provided the auxiliary subsystem ${}^{C}D^{\theta,\vartheta,\zeta} e^2 = \sum_s \beta_s A_s^{22} e^2$ is, itself, generalized Mittag–Leffler stable, i.e., under a detectability-type condition on the auxiliary dynamics. This is the case in the numerical example, where $A_s^{21} = 0$ and the eigenvalues of A_1^{22} and A_2^{22} are $-0.50 \pm 0.99\,i$ and $-0.65 \pm 0.98\,i$ (both with negative real parts), so e^2 is decoupled from e^1 and converges, as confirmed by the numerical example of Section 5. Conversely, if some A_s^{22} were unstable, then L_s^2 would be needed, and the choice $L_s^2 = 0$ could lead to divergence or a convergence lag of e^2 even though e^1 stays practically stable; in that situation, L_s^2 should be designed (for instance, by a second SOS condition on $A_s^{22} - L_s^2 C_2$) to stabilize or accelerate the auxiliary error. This clarifies the precise sense in which L_s^2 may be set to zero.

5. Simulation Results

In this section, we present a numerical example to illustrate the effectiveness of the proposed polynomial fuzzy observer design and to support the theoretical findings established in Theorem 2. To improve readability, all figures reported below have been redrawn with substantially enlarged fonts, thicker curves and explicit markers so that the characters and the curves are clearly legible.

Consider a 3-dimensional tempered fractional-order polynomial fuzzy system of the form (17) with $n = 3$, decomposed into the state of interest $x^1 \in \mathbb{R}$ ($n_1 = 1$) and the auxiliary dynamics $x^2 \in \mathbb{R}^2$ ($n_2 = 2$). The measured output is

$$ y(\varsigma) = x_1(\varsigma), $$

which implies $C_1 = 1$. The fractional order is chosen as

$$ \theta = 0.90, $$

the tempering parameter as

$$ \vartheta = 0.15, $$

and the function $\zeta(\varsigma)$ is taken as

$$ \zeta(\varsigma) = \varsigma. $$

The system operates with $f = 2$ fuzzy rules, using the premise variable $y(\varsigma)$. The membership functions are defined by

$$ \beta_1(y(\varsigma)) = \frac{1}{1 + y^2(\varsigma)}, \qquad \beta_2(y(\varsigma)) = \frac{y^2(\varsigma)}{1 + y^2(\varsigma)}. $$

The polynomial system matrices for Rule 1 are

$$ A_1^{11}(y) = -1.80 - 0.20 y^2, \qquad A_1^{12}(y) = \omega \begin{bmatrix} 0.10 & 0.03(1 + y^2) \end{bmatrix}, $$

$$ A_1^{21}(y) = \begin{bmatrix} 0 \\ 0 \end{bmatrix}, \qquad A_1^{22}(y) = \begin{bmatrix} -0.35 & 1.00 \\ -1.00 & -0.65 \end{bmatrix}. $$

For Rule 2, the matrices are

$$A_2^{11}(y) = -1.40 - 0.10y^2, \qquad A_2^{12}(y) = \omega\begin{bmatrix}0.08 & 0.02(1+y^2)\end{bmatrix},$$
$$A_2^{21}(y) = \begin{bmatrix}0\\0\end{bmatrix}, \qquad A_2^{22}(y) = \begin{bmatrix}-0.45 & 1.00\\-1.00 & -0.85\end{bmatrix}.$$

The nonlinear perturbation terms, which satisfy Assumption 1, are defined as

$$\phi_1(\varsigma, x, \omega) = \omega\begin{bmatrix}0.18\sin(x_1)\\0.04\sin(x_1)\\0\end{bmatrix}, \qquad \phi_2(\varsigma, x, \omega) = \omega\begin{bmatrix}0.14\sin(x_1)\\0.03\sin(x_1)\\0\end{bmatrix}.$$

The small parameter is fixed at

$$\omega = 0.20,$$

and the compact operating region is chosen as

$$\mathcal{Y} = [-2.0, 2.0].$$

To design the polynomial fuzzy observer (20)–(21), we choose

$$\eta = 1.0, \qquad P = 1.0.$$

The primary objective is to determine the gains $L_s^1(y)$ such that the first-block design condition associated with (24) is satisfied on $\mathcal{Y}$. The values $\eta = 1$ and $P = 1$ are selected so that this SOS condition is feasible with a comfortable margin on $\mathcal{Y}$, as quantified below. As discussed in Section Discussion: Design Parameters and Structural Assumptions, a larger η would increase the certified decay rate $\alpha = \eta/(2\lambda_{\max}(P))$ and tighten the ultimate bound, but would make (24) harder to satisfy and require larger gains, whereas a smaller η relaxes the design at the price of slower convergence; $\eta = 1$ realizes a balanced choice here.

By selecting the polynomial observer gains for the first state component as

$$L_1^1(y) = 0.90 + 0.05y^2, \qquad L_2^1(y) = 1.00 + 0.03y^2,$$

the sampled first-block negativity condition associated with (24), namely

$$2\left(A_s^{11}(y) - L_s^1(y)\right) + \eta < 0,$$

is satisfied on $y \in [-2.0, 2.0]$. More precisely, the corresponding polynomial expression attains a maximum value of

$$-3.800000$$

and a minimum value of

$$-6.400000$$

over $\mathcal{Y}$. Since the maximum value is strictly negative, the sampled first-block design inequality is numerically satisfied on the admissible operating region $\mathcal{Y}$. The gains for the auxiliary dynamics are selected as

$$L_1^2(y) = L_2^2(y) = \begin{bmatrix}0\\0\end{bmatrix},$$

in accordance with Remark 3. The numerical outputs also show that the measured output remains inside the operating region, with

$$\max_{\varsigma\in[0,10]} |y(\varsigma)| = 1.000000 < 2,$$

which confirms that the trajectory stays within $\mathcal{Y}$.

Furthermore, Theorem 2 requires the integral kernel map (25) to be bounded. Its numerical evaluation yields

$$\sup_{\varsigma\in[0,10]} K(\varsigma) \approx 1.589735.$$

As illustrated in Figure 2, the kernel-boundedness diagnostic increases and then approaches a finite plateau, which is consistent with the boundedness assumption used in the theorem.

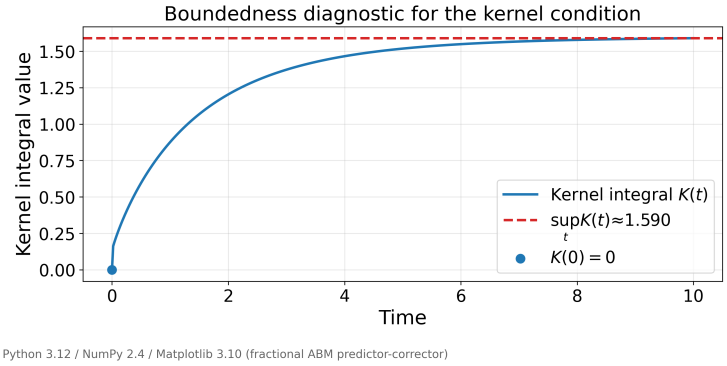

Figure 2. Evolution of the kernel integral map associated with the boundedness condition (25). The initial value $K(0) = 0$ and the supremum $\sup_\varsigma K(\varsigma) \approx 1.59$ are indicated; enlarged fonts are used, and the figure was generated in Python 3.12/Matplotlib.

The system and observer are simulated over the interval

$$\varsigma \in [0, 10]$$

with time step

$$h = 0.02,$$

using a fractional Adams–Bashforth–Moulton predictor–corrector method applied after the standard exponential transformation associated with the tempered Caputo dynamics. To ensure reproducibility, we specify the solver, precision and termination conditions explicitly: the predictor–corrector scheme uses $N = \lceil (t_f - t_0)/h \rceil = 500$ uniform steps and applies, at each step, one predictor evaluation followed by one corrector evaluation (a $P(EC)$ structure), so that no inner iterative loop—and hence, no iteration tolerance—is involved; all computations are carried out in IEEE-754 double-precision arithmetic; the one- and two-parameter Mittag–Leffler functions entering the theoretical bound (26) and the kernel diagnostic (25) are evaluated by their defining series truncated when the current term falls below 10^{-13} in absolute value (at most 400 terms); and the integration is terminated at the fixed final time $\varsigma = 10$. All computations and figures were produced in Python 3.12 (NumPy 2.4, Matplotlib 3.10); this platform, together with the solver above, is reported so that the experiment can be reproduced exactly. The initial conditions are chosen as

$$x(0) = \begin{bmatrix} 1.0 & -0.8 & 0.6 \end{bmatrix}^T, \qquad \hat{x}(0) = \begin{bmatrix} 0.0 & 0.0 & 0.0 \end{bmatrix}^T,$$

which yields the initial estimation error

$$e(0) = \begin{bmatrix} 1.0 & -0.8 & 0.6 \end{bmatrix}^T.$$

Figure 3 displays the time evolution of the plant states and their corresponding estimates. The output trajectory remains inside the admissible set $\mathcal{Y}$ throughout the simulation, which confirms Assumption 1(H4).

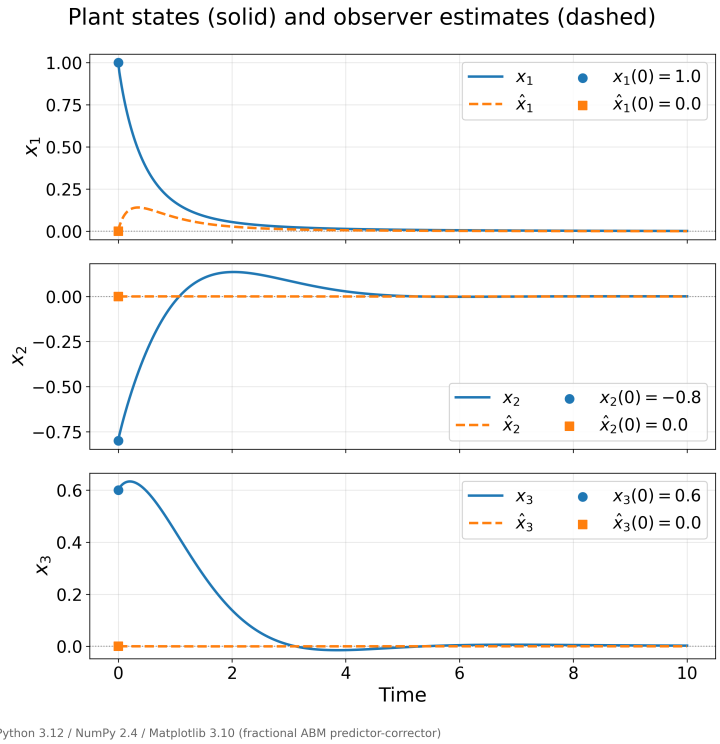

Figure 3. Trajectories of the plant states $x(\varsigma)$ (solid lines) and the observer estimates $\hat{x}(\varsigma)$ (dashed lines). The initial conditions $x(0) = (1, -0.8, 0.6)$ and $\hat{x}(0) = (0, 0, 0)$ are marked, and the zero reference line is shown; enlarged fonts are used, and the figure was generated in Python 3.12/Matplotlib.

The dynamics of the estimation error

$$e(\varsigma) = x(\varsigma) - \hat{x}(\varsigma)$$

are shown in Figure 4. The upper subplot highlights the main conclusion of Theorem 2: the absolute error of the first component $|e_1(\varsigma)|$ remains below the theoretical Mittag–Leffler decay envelope (26). In particular, at the final time $\varsigma = 10$, the actual error satisfies

$$|e_1(10)| \approx 1.219 \times 10^{-3},$$

whereas the theoretical estimate gives

$$1.067 \times 10^{-1}.$$

Thus, the theoretical bound is respected and is conservative, as expected from a Lyapunov-based practical stability estimate. The roughly two-order-of-magnitude gap between the guaranteed bound 1.067×10^{-1} and the actual error 1.219×10^{-3} deserves an explicit comment. It is the cumulative effect of several worst-case steps in the analysis: (i) the comparison lemma replaces the true, oscillatory and sign-varying, error dynamics by their monotone Mittag–Leffler majorant; (ii) Young's inequality in (30)–(32) over-bounds

the cross term $2\lambda_{\max}(P)\delta_2(\omega)\mu(\varsigma)\|e^1\|$; and (iii) the perturbation is handled through its uniform bound $\delta_2(\omega)\mu(\varsigma)$ rather than its much smaller instantaneous value. Here, the conditioning prefactor $\sqrt{\lambda_{\max}(P)/\lambda_{\min}(P)} = 1$ (because $P = 1$) contributes nothing, so the gap originates entirely from steps (i)–(iii). The gap therefore measures *guaranteed robustness* and is intrinsic to Lyapunov-based practical estimates, not a looseness of the simulation. It can be narrowed by optimizing P and η (e.g., maximizing η subject to (24)), by sharpening the constants δ_1, δ_2, or by replacing the scalar comparison estimate with a less conservative weighted/vector Lyapunov argument; these refinements are left for future work. The complete final estimation error is

$$e(10) = \begin{bmatrix} 0.00121908 & 0.00085852 & 0.00243679 \end{bmatrix}^T.$$

The auxiliary error components e_2 and e_3 also decay numerically toward zero in this example, although Theorem 2 only guarantees practical generalized Mittag–Leffler stability with respect to e^1.

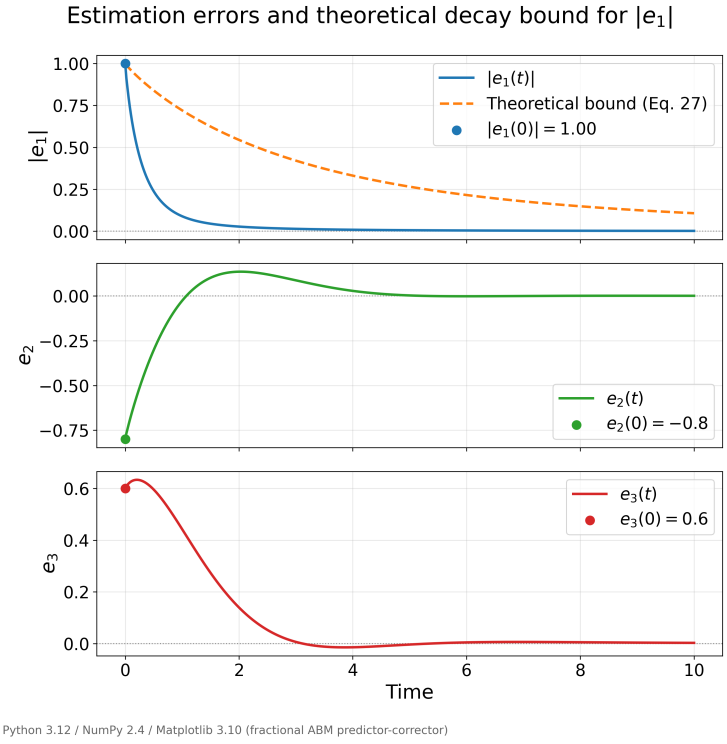

Figure 4. Time evolution of the estimation errors e_1, e_2, and e_3, together with the theoretical decay bound for $|e_1(\varsigma)|$ given by (26). The initial errors $e(0) = (1, -0.8, 0.6)$ are marked, and the zero reference line is shown, so that the convergence to 0 is explicit; enlarged fonts are used, and the figure was generated in Python 3.12/Matplotlib.

Finally, Figure 5 shows the evolution of the fuzzy membership functions during the simulation. The first weight $\beta_1(y(\varsigma))$ rapidly becomes dominant as $y(\varsigma)$ approaches the origin, while $\beta_2(y(\varsigma))$ decreases toward zero. This indicates that the closed-loop behavior is progressively governed by the first local model as the state converges.

Overall, the numerical results are in excellent agreement with Theorem 2 and strongly support the conclusion that the estimation error system is $\bar{\omega}$-ζ-practically uniformly generalized Mittag–Leffler stable with respect to e^1.

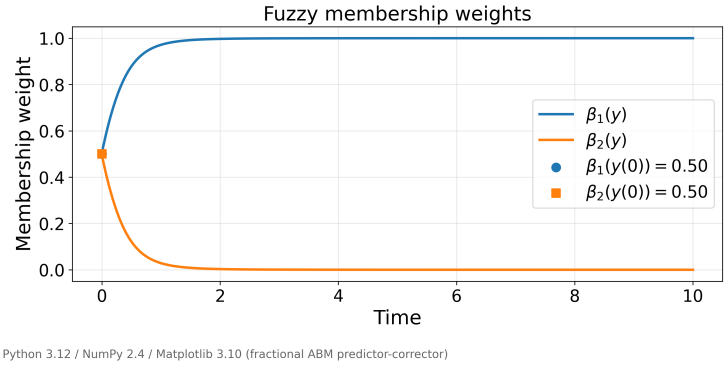

Figure 5. Evolution of the fuzzy membership weights $\beta_1(y)$ and $\beta_2(y)$ depending on the measured output $y(\varsigma)$. Initial values $\beta_1(y(0))$ and $\beta_2(y(0))$ are marked; enlarged fonts are used, and the figure was generated in Python 3.12/Matplotlib.

Comparison with previous works and quantitative assessment. It is instructive to contrast the proposed scheme with existing observers for fractional and tempered fuzzy systems. Full-state designs, such as the fractional-order polynomial fuzzy observers of [25], the H_∞ fuzzy fractional observers of [26], and the nonlinear tempered fractional observers of [24], certify the *entire* estimation error and therefore require a Lyapunov certificate and gain blocks covering all state components. In contrast, the present partial design certifies only the substate of interest e^1 and uses a single gain block L_s^1, leaving L_s^2 free; this reduces the number of design variables and the conservatism associated with simultaneously dominating the auxiliary dynamics. Quantitatively, on the three-dimensional example, the certified component reaches $|e_1(10)| \approx 1.22 \times 10^{-3}$ while remaining below the guaranteed envelope 1.07×10^{-1}, the output never leaves the operating region ($\max_\varsigma |y(\varsigma)| = 1 < 2$), and the kernel diagnostic stays bounded ($\sup_\varsigma K(\varsigma) \approx 1.59$). These figures show that accurate substate estimation is achieved at a reduced design cost. The structural differences between the proposed scheme and representative existing designs are summarized in Table 1. A fully numerical benchmark against full-state tempered fractional fuzzy observers on a common plant is a natural next step, noting that such observers are not directly applicable to the present partial-estimation setting.

Table 1. Structural comparison of the proposed observer with representative existing designs.

Reference	Operator	Model Class	Design Tool	Certified Objective/Gains
[25]	Caputo (parameter-dependent)	polynomial fuzzy	SOS	full-state estimation error; full observer gain
[26]	Hadamard	T–S fuzzy	LMI (H_∞)	full-state, H_∞ observer-based control; full gain
[27]	Caputo	T–S fuzzy with unknown inputs	LMI (Thau–Luenberger)	full-state estimation error; full gain
[24]	tempered Caputo	nonlinear (non-fuzzy)	matrix inequalities	full-state estimation error; full gain
[28]	tempered Caputo	nonlinear fuzzy	Lyapunov conditions	practical stabilization (control, no observer)
This work	tempered ζ-Caputo	polynomial fuzzy	SOS on compact region $\mathcal{Y}$	partial: practical generalized ML stability of e^1 only; single gain block L_s^1 (L_s^2 free)

6. Conclusions

This paper has investigated the problem of partial practical stability for a class of tempered fractional-order systems described by the tempered ζ-Caputo derivative. A general Lyapunov-based criterion has been established to guarantee practical uniform generalized Mittag–Leffler stability with respect to a prescribed state component. In this framework, the stability objective does not concern the full state vector, but rather a substate of interest, which makes the proposed approach particularly suitable for reduced-order regulation

and estimation problems. Based on the developed theoretical result, a polynomial fuzzy observer has been designed for a class of tempered fractional-order nonlinear systems. By exploiting a block decomposition of the state and estimation error, and by constructing a Lyapunov function depending only on the first error component, sufficient conditions have been obtained to ensure practical generalized Mittag–Leffler stability of the estimation error with respect to e^1. The observer synthesis conditions were expressed in terms of polynomial matrix inequalities and sum-of-squares constraints on a compact admissible operating region. The numerical example has illustrated the effectiveness of the proposed approach. In particular, the simulation results confirmed that the estimation error component of interest remains below the theoretical Mittag–Leffler decay bound and converges toward a small neighborhood of the origin, which is in agreement with the developed theory. This demonstrates the relevance of the proposed framework for observer design in nonlinear tempered fractional-order fuzzy systems. Despite these advantages, the proposed approach has several drawbacks that should be acknowledged. First, the guarantees are *partial*: only the substate e^1 is certified, and convergence of the auxiliary error e^2 requires the separate (detectability-type) stability of the matrices A_s^{22} when the auxiliary gain L_s^2 is set to zero. Second, the analysis rests on a quadratic Lyapunov function ($\iota = 2$) and on the measurable-premise assumption (H1), which restrict the admissible model class and introduce conservatism, as quantified by the two-order-of-magnitude gap between the theoretical and the actual error. Third, the SOS/polynomial-matrix-inequality synthesis, although convex, scales unfavorably with the dimension n_1 and the polynomial degree, and the nonlocal nature of the tempered fractional operator makes long-horizon simulation computationally demanding ($\mathcal{O}(N^2)$ per run). These drawbacks delineate the scope of the method and directly motivate the extensions listed next. Possible directions for future work include the extension of the present framework to output-feedback control, observer-based control under input saturation or disturbances, delayed tempered fractional-order systems, and variable-order or distributed-order tempered operators. Another promising perspective is the development of less conservative full-state extensions and computationally efficient numerical schemes for high-dimensional tempered fractional-order observer design.

Author Contributions: Conceptualization, A.R.A.A. and A.B.M.; methodology, O.N. and A.B.M.; software, O.N.; validation, A.R.A.A., R.F. and O.N.; formal analysis, R.F. and A.B.M.; investigation, A.R.A.A. and R.F.; resources, R.F.; data curation, O.N.; writing—original draft preparation, O.N. and A.B.M.; writing—review and editing, A.R.A.A. and R.F.; visualization, O.N.; supervision, A.B.M.; project administration, R.F.; funding acquisition, A.R.A.A. and R.F. All authors have read and agreed to the published version of the manuscript.

Funding: This work was funded by the Deanship of Graduate Studies and Scientific Research at Jouf University under grant No. (DGSSR-2025-02-01166).

Data Availability Statement: The original contributions presented in this study are included in the article. Further inquiries can be directed to the corresponding authors.

Conflicts of Interest: The authors declare no conflicts of interest. The funders had no role in the design of the study; in the collection, analyses, or interpretation of data; in the writing of the manuscript; or in the decision to publish the results.

References

1. Podlubny, I. *Fractional Differential Equations*; Academic Press: San Diego, CA, USA, 1999.
2. Kilbas, A.A.; Srivastava, H.M.; Trujillo, J.J. Theory and Applications of *Fractional Differential Equations*; Elsevier: Amsterdam, The Netherlands, 2006.

3. Ben Makhlouf, A. On the stability of caputo fractional-order systems: A survey. In *Fractional Order Systems—Control Theory and Applications*; Springer: Cham, Switzerland, 2021; pp. 1–8.
4. Sadek, L.; Sadek, O.; Alaoui, H.T.; Abdo, M.S.; Shah, K.; Abdeljawad, T. Fractional order modeling of predicting COVID-19 with isolation and vaccination strategies in morocco. *Comput. Model. Eng. Sci.* **2023**, *136*, 1931–1950. [CrossRef]
5. Abouelregal, A.E.; Alhassan, Y.; Alsaeed, S.S.; Elzayady, M.E. Tempered fractional thermal conduction model for magnetoelastic solids with spherical holes under time-dependent laser pulse heating. *Arch. Appl. Mech.* **2025**, *95*, 27. [CrossRef]
6. Balegh, M.; Ghezal, A. Theoretical analysis and applications of fixed-point theorems in delay fractional differential equations. *J. Appl. Math. Comput.* **2025**, *71*, 867–881. [CrossRef]
7. Attia, N.; Akgül, A.; Seba, D.; Nour, A. An efficient numerical technique for a biological population model of fractional order. *Chaos, Solitons Fractals* **2020**, *141*, 110349. [CrossRef]
8. Ghezal, A.; Al Ghafli, A.A.; Al Salman, H.J. Anomalous drug transport in biological tissues: A Caputo fractional approach with non-classical boundary modeling. *Fractal Fract.* **2025**, *9*, 508. [CrossRef]
9. Deng, J.; Ma, W.; Deng, K.; Li, Y. Tempered mittag-leffler stability of tempered fractional dynamical systems. *Math. Probl. Eng.* **2020**, *2020*, 7962542. [CrossRef]
10. Medved, M.; Pospisil, M. Generalized laplace transform and tempered ψ-caputo fractional derivative. *Math. Model. Anal.* **2023**, *28*, 146–162. [CrossRef]
11. Li, C.; Deng, W.; Zhao, L. Well-posedness and numerical algorithm for the tempered fractional differential equations. *Discret. Contin. Dyn. Syst. Ser. B* **2019**, *24*, 1989–2015. [CrossRef]
12. Almeida, R.; Martins, N.; Sousa, J.V.d.C. Fractional tempered differential equations depending on arbitrary kernels. *Aims Math.* **2024**, *9*, 9107–9127. [CrossRef]
13. Ben Makhlouf, A.; Alkhrijah, Y.; Ben Makhlouf, A. Practical stability and robust state-feedback for tempered ϑ-caputo fractional systems. *Int. J. Syst. Sci.* **2026** , 1–11. [CrossRef]
14. Lamrani, I.; Zitane, H.; Torres, D.F.M. Controllability and observability of tempered fractional differential systems. *Commun. Nonlinear Sci. Numer. Simul.* **2025**, *142*, 108501. [CrossRef]
15. Gao, D.; Qiu, Z.; Wang, L.; Li, J. A simple and effective second-order numerical algorithm for tempered fractional differential equation with time caputo-tempered fractional derivative. *Adv. Math. Phys.* **2025**, *2025*, 5518224. [CrossRef]
16. Zaky, M.A.; Doha, E.H. A new adaptive spectral collocation method for tempered fractional differential equations with initial singularities. *Comput. Appl. Math.* **2026**, *45*, 302. [CrossRef]
17. Benabdallah, A.; Ellouze, I.; Hammami, M.A. Practical exponential stability of perturbed triangular systems and a separation principle. *Asian J. Control* **2011**, *13*, 445–448. [CrossRef]
18. Ghanmi, B. Stability of impulsive systems depending on a parameter. *Math. Methods Appl. Sci.* **2016**, *39*, 2626–2646. [CrossRef]
19. Ghanmi, B. On the practical *h*-stability of nonlinear systems of differential equations. *J. Dyn. Control Syst.* **2019**, *25*, 691–713. [CrossRef]
20. Hamzaoui, A.; Hadj Taieb, N.; Hammami, M.A. Practical partial stability of time-varying systems. *Discret. Contin. Dyn.-Syst. Ser. B* **2022**, *27*, 3585–3603. [CrossRef]
21. Dorgham, A.; Hammami, M.A. Practical tracking control of a class of uncertain nonlinear systems with unknown output function. *Int. J. Adapt. Control Signal Process.* **2023**, *37*, 2434–2450. [CrossRef]
22. Damak, H.; Hammami, M.A.; Maaloul, K. Observers based control for stabilization of non-autonomous evolution equations in banach spaces. *Complex Anal. Oper. Theory* **2023**, *17*, 65. [CrossRef]
23. Alawad, M.A. Lyapunov-based analysis of partial practical stability in tempered fractional calculus. *Fractal Fract.* **2025**, *9*, 716. [CrossRef]
24. Alawad, M.A.; Louhichi, B. Innovative observer design for nonlinear tempered fractional-order systems. *Asian J. Control* **2026**, *28*, 361–368. [CrossRef]
25. Gassara, H.; Rhaima, M.; Mchiri, L.; Ben Makhlouf, A. Observer design for fractional-order polynomial fuzzy systems depending on a parameter. *Fractal Fract.* **2024**, *8*, 693. [CrossRef]
26. Rhaima, M.; Gassara, H.; Mchiri, L.; El Hajjaji, A.; Ben Makhlouf, A. H_∞ observer-based control for fuzzy hadamard fractional-order systems. *Comput. Appl. Math.* **2025**, *44*, 194. [CrossRef]
27. Djeddi, A.; Azar, A.T.; Ahmed, S.; Dib, J.; Kamal, N.A.; Haider, Z. Fractional order thau-luenberger observer for fractional order takagi-sugeno dynamical systems under uncertain nonmeasurable variables and unknown inputs. *Aims Math.* **2025**, *10*, 15108–15130. [CrossRef]
28. Rguigui, H.; Elghribi, M. Practical stabilization for a class of tempered fractional-order nonlinear fuzzy systems. *Asian J. Control* **2026**, *28*, 294–300. [CrossRef]

29. Gassara, H.; Kharrat, D.; Ben Makhlouf, A.; Mchiri, L.; Rhaima, M. Sos approach for practical stabilization of tempered fractional-order power systems. *Mathematics* **2023**, *11*, 3024. [CrossRef]
30. Hui, J.; Yuan, J. Adaptive second-order nonsingular terminal sliding mode power-level control for nuclear power plants. *Nucl. Eng. Technol.* **2022**, *54*, 1644–1651. [CrossRef]

Disclaimer/Publisher's Note: The statements, opinions and data contained in all publications are solely those of the individual author(s) and contributor(s) and not of MDPI and/or the editor(s). MDPI and/or the editor(s) disclaim responsibility for any injury to people or property resulting from any ideas, methods, instructions or products referred to in the content.